Semicond. Sci. Technol. **13** (1998) A130–A134. Printed in the UK PII: S0268-1242(98)91835-1

Experimental demonstration of quantum-dot cellular automata

G L Snider, A O Orlov, I Amlani, G H Bernstein, C S Lent, J L Merz and W Porod

Department of Electrical Engineering, University of Notre Dame, Notre Dame, IN 46556, USA

Received 7 December 1997, accepted for publication 11 March 1998

Abstract. We present the experimental demonstration of a basic cell of quantum-dot cellular automata (QCA), a transistorless computation paradigm which addresses the issues of device density and interconnection. The device presented is a six-dot quantum-dot cellular system consisting of a four-dot QCA cell and two electrometer dots. The system is fabricated using metal dots which are connected by capacitors and tunnel junctions. The operation of a basic cell is confirmed by the externally controlled polarization change of the cell. The cell exhibits a bistable response, with more than 80% polarization of the charge within a cell.

1. Introduction

For more than 30 years the microelectronics industry has enjoyed dramatic improvements in the speed and size of electronic devices, and continued growth in the industry requires a further increase in the number of devices fabricated on a chip. This trend has long obeyed Moore's law, which predicts that the number of devices integrated on a chip will double every 18–24 months. Adherence to this exponential growth curve has been a monumental task requiring rapid improvements in all aspects of integrated circuit fabrication, permitting manufacturers both to shrink the size of devices and to increase chip size while maintaining acceptable yields. Since the early 1970s the device of choice for high levels of integration has been the field effect transistor (FET), and while the FET of today is a vast improvement over that of 1970, it is still a current switch like the mechanical relays first used to encode binary information. At gate lengths below 0.1 μm, FETs will begin to encounter fundamental effects which make further scaling difficult. A possible method for the microelectronics industry to maintain continued growth in device density is to change from the FET-based paradigm to one based on nanostructures. Here, instead of fighting the effects that come with feature size reduction, these effects are used to advantage. One nanostructure paradigm, proposed by Lent *et al* [1, 2], is quantum-dot cellular automata (QCA), which employs arrays of coupled quantum dots to implement Boolean logic functions [3, 4]. The advantage of QCA lies in the extremely high packing densities possible due to the small size of the dots, the simplified interconnection and the extremely low power–delay product which can be arbitrarily reduced by adiabatic switching [5]. Using QCA cells with dots of 20 nm diameter, an entire full adder can be placed within 1 μm^2, approximately the area of a single 0.07 μm gate length FET.

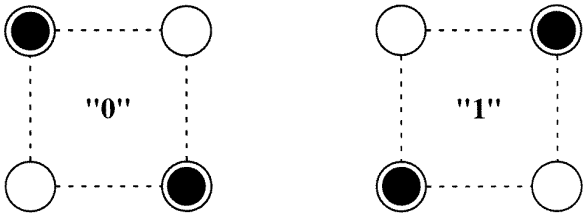

Figure 1. Basic four-dot QCA cell showing the two possible polarizations.

A basic QCA cell consists of four quantum dots located at the corners of a square, coupled by tunnel barriers. If the cell is biased so that there are two excess electrons among the four dots, Coulomb repulsion will force the electrons to opposite corners. There are thus two energetically equivalent polarizations, as shown in figure 1. These two polarizations can be labelled logic '0' and '1', and, by properly arranging cells so that the polarization of one cell sets the polarization of a nearby cell, it is possible to implement all combinational logic functions. A tremendous advantage of QCA devices is the simplified interconnect which is possible with this paradigm. Since the cells communicate only with their nearest neighbours, there is no need for long interconnect lines. The inputs are applied to the cells at the edge of the system and the computation proceeds until the output appears at cells at the edge of the QCA array.

2. Experiment

The experimental work presented is based on a QCA cell using aluminium islands with aluminium oxide tunnel junctions, fabricated on an oxidized silicon wafer. The fabrication used standard electron beam lithography and shadow evaporation to form the islands and tunnel

0268-1242/98/SA0130+05$19.50

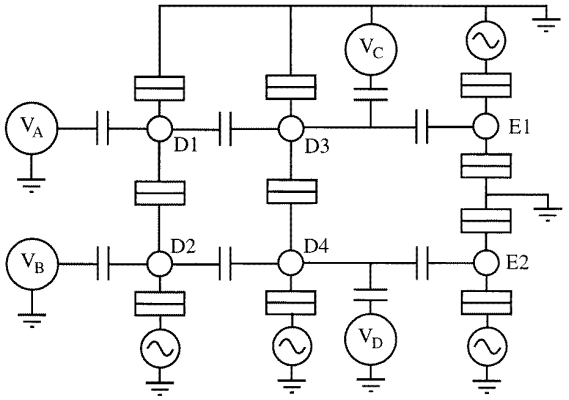

Figure 2. Schematic diagram of the four-dot QCA cell with two electrometers.

junctions [6]. The area of the tunnel junctions is an important quantity since this dominates island capacitance, determining the charging energy of the island and hence the operating temperature of the device. For our devices the area is approximately 50 nm by 50 nm, giving a junction capacitance of 240 aF.

We recently demonstrated the first step in the development of QCA systems, i.e. a functional QCA cell where we can switch the polarization of a cell, confirming that the switching of a single electron between coupled quantum dots can control the position of a single electron in a second set of dots [7]. A schematic diagram of our four-dot QCA cell with additional electrometers is shown in figure 2. The four dots of the QCA cell consist of two double dots, where the dots are joined by a tunnel junction. This breaks the QCA cell into two half-cells, where electrons are allowed to tunnel 'vertically' between dots but not 'horizontally'. The input voltages V_A and V_B are connected to double dot D1 and D2, which form the input half-cell. These are connected capacitively to the output half-cell D3 and D4, which are in turn capacitively coupled to the electrometers E1 and E2. The circuit was mounted on the cold finger of a dilution refrigerator whose base temperature is 10 mK. The conductance through each double-dot half-cell and each individual electrometer can be measured simultaneously using standard ac lock-in techniques. An excitation voltage of 4 μV was typically used, with a frequency between 16 and 40 Hz. A magnetic field of 1 T was applied to suppress the superconductivity of the aluminium metal. The capacitances between the gates and islands were extracted from the period of the Coulomb blockade oscillations [8].

The operation of a QCA cell is best understood by examining the conductance through the output half-cell as a function of the two gate voltages V_C and V_D, as shown in the contour plot of figure 3. A peak in the conductance is observed each time the Coulomb blockade is lifted for the double-dot system, and because of the capacitive coupling between the dots each peak splits into a double peak. These peaks form the vertices of a hexagonal structure which we refer to as the 'honeycomb', delineated by the broken lines in figure 3 [9]. The electron population of the dots is stable within each hexagon of the honeycomb and changes when

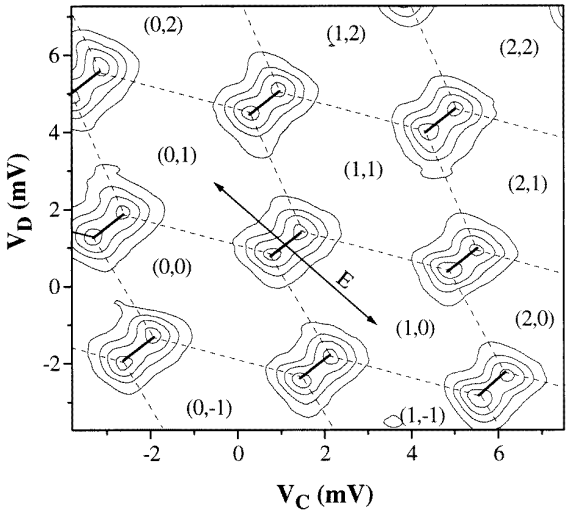

Figure 3. Contour plot of the measured conductance through the output half-cell as a function of V_C and V_D. The excess electron population is noted as (n_3, n_4).

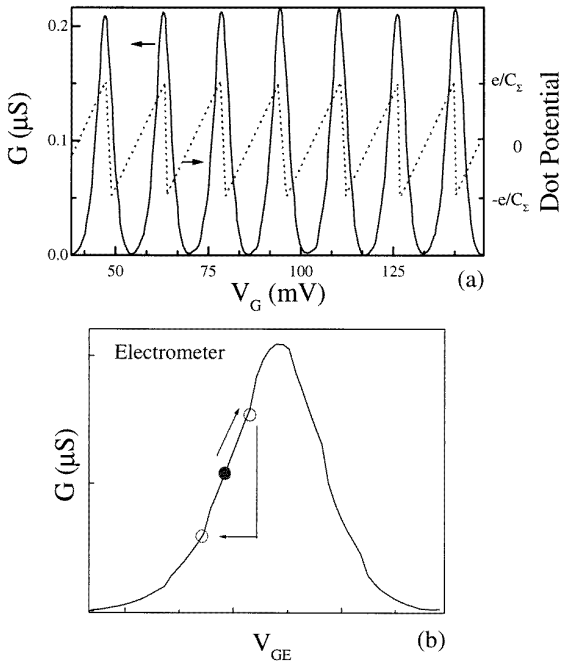

Figure 4. (*a*) The measured conductance and calculated potential of a single dot as a function of its gate bias. (*b*) A single conductance peak of the electrometer dot, as a function of its gate bias. The nominal working point is set to the left side of the peak, and the potential variations on the coupled dot cause excursions away from this point, causing large changes in the electrometer conductance.

a border between cells is crossed. The excess electron population within each hexagon can thus be labelled, with the $(0, 0)$ hexagon centred at $V_C = V_D = 0$ V. A point in the honeycomb defined by a single setting of V_C and V_D is called the working point, which defines a particular configuration of electrons. If V_C is swept in the positive direction with V_D fixed, electrons are added one by one to the top dot as the working point moves horizontally through the hexagons $(1, 0)$ then $(2, 0)$ and so on. If V_D is

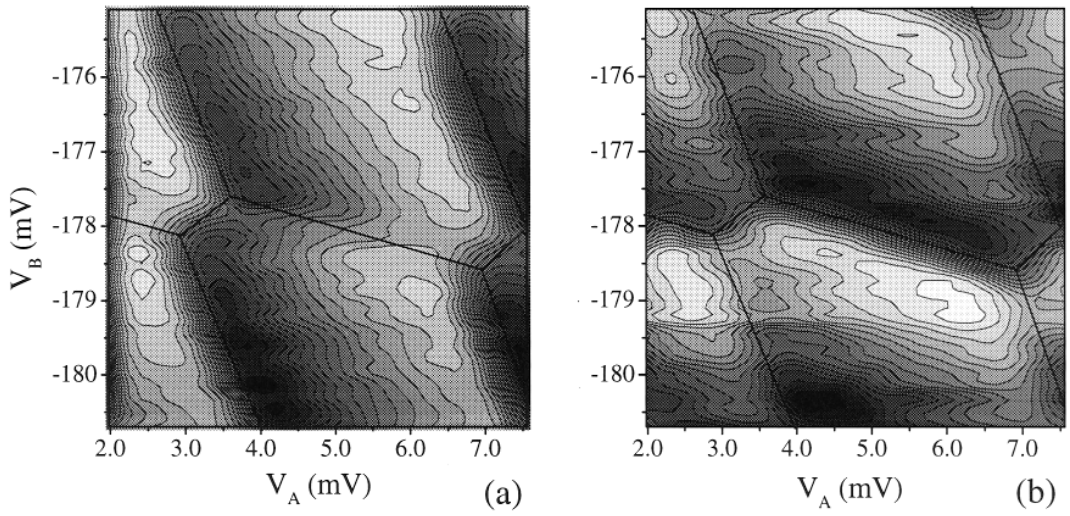

Figure 5. (*a*) Contour plot of the conductance through electrometer E1 as a function of V_C and V_D. Light regions represent areas of high conductance and dark regions those of low conductance. (*b*) Contour plot of the conductance through electrometer E2.

swept positive, electrons are added to the bottom dot as the working point moves vertically through the hexagons (0, 1) and (0, 2). Most important for QCA operation is motion of the working point in the direction shown by arrow E in figure 3. This movement between the (0, 1) and (1, 0) hexagon represents the switching of an electron between the bottom dot and top dot. The goal of our experiment is to demonstrate QCA operation by using electrodes to force this transition in the input half-cell and then to have the potential changes on the input half-cell force an opposite transition in the output half-cell.

Since the operation of a QCA cell depends on the position of a single electron, it is necessary to track the positions of electrons within the cell. One way to do this is to measure the conductance through each half-cell. A peak in the conductance as the gate voltages are changed indicates that the Coulomb blockade has been lifted for both dots simultaneously, and a change in the dot population has occurred. However, as seen in figure 3, not all electron transitions can be detected in this manner. If V_C alone is swept, electrons are added to only the top dot, and no change in the conductance through the dots is seen. To characterize fully the QCA cell it is therefore necessary to detect externally the charge state of each dot individually. This is done using additional dots as electrometers [10], capacitively coupled to the output half-cell, as shown in the schematic of figure 2. The electrometer operates by detecting small potential changes in the dot being measured. Figure 4(*a*) plots the measured dot conductance and theoretical potential as a function of an applied gate voltage. The potential on a dot exhibits a sawtooth behaviour, increasing with positive gate voltage, followed by an abrupt reset when an additional electron is added to the dot. For the dots used in our experiments, the amplitude of this sawtooth oscillation is approximately 110 μV. The operation of the electrometer is shown in figure 4(*b*), which expands a single conductance peak. The gate voltage of the electrometer is adjusted so that the working point lies on the side of one of the conductance peaks and is then held constant through the rest of the experiment. Any potential variations coupled to the electrometer, such as those on a nearby dot, will act as an additional gate voltage to the electrometer dot which causes a shift of the working point shown in figure 4(*b*). Since the conductance peaks are quite sharp, a small change in the gate voltage gives a large change in the conductance through the electrometer dot. Knowing the capacitance coupling the electrometer to the dot and the shape of the electrometer conductance peak, it is possible to calculate the potential on the measured dot. In these measurements it is important to know which side of the conductance peak is chosen for the electrometer working point since the sign of the transconductance changes from side to side. In our experiments the electrometers are always biased on the left side of the peak, giving a positive transconductance.

Figure 5, which shows a contour plot of the conductance through each of the electrometers, demonstrates that the electrometers can externally detect the movement of an electron in a double-dot half-cell. Figure 5(*a*) shows the conductance of the top electrometer as a function of V_C and V_D. The overlying lines show the honeycomb borders as determined by a simultaneous measurement of the conductance through the double dot. It is clearly seen that the largest changes in the electrometer conductance occur at the honeycomb borders where electrons are added to D3. Only a small change is seen when electrons are added to D4, because of the unavoidable, but small, parasitic capacitance coupling the upper electrometer to D4. Similarly, the conductance through the lower electrometer shows a large change when electrons are added to D4, as shown in figure 5(*b*). In each case the conductance through the electrometer is proportional to the potential on the corresponding dot. In our experiments we typically use both the conductance through each half-cell and the electrometer signals to characterize completely the operation of the QCA cell.

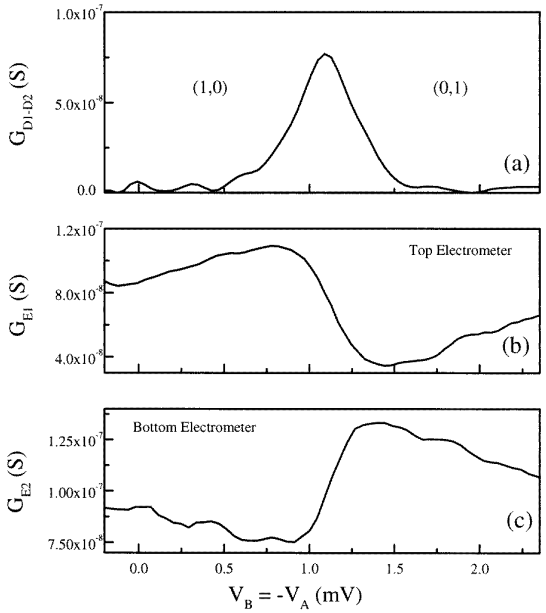

Figure 6. (*a*) Conductance through the input half-cell, where the peak indicates the switch of an electron from D1 to D2. (*b*) Conductance through the electrometer E1 indicating the addition of an electron to D3. (*c*) Conductance through electrometer E2 indicating the removal of an electron from D4.

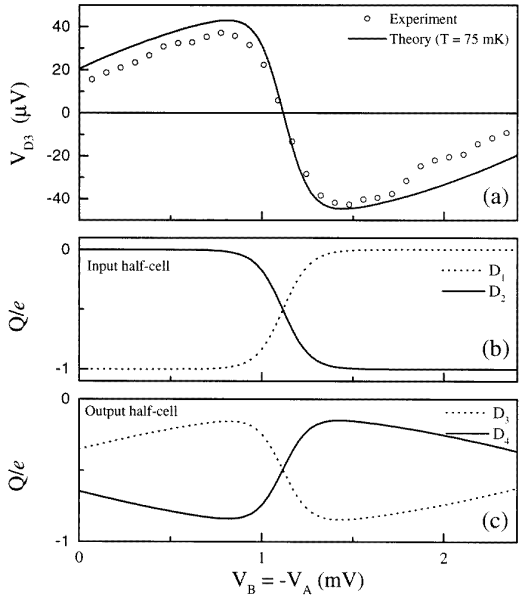

Figure 7. (*a*) Measured potential on dot D3 as a function of the differential input $V_B = -V_A$ together with theory at 75 mK. Calculated excess electron populations for (*b*) the input half-cell D1 and D2 and (*c*) the output half-cell D3 and D4 as a function of the differential input are also shown.

QCA operation is demonstrated by applying a differential voltage to the input half-cell, a positive bias to V_B and a negative bias to V_A. As this differential voltage is swept, electrons are moved one by one from D1 to D2, and the electrostatic potential on D1 and D2 changes in response to the applied gate voltages and the position of electrons. The potential on D2 increases with the positive voltage V_B, until an abrupt reset which occurs when an electron enters the dot, corresponding to the sawtooth pattern seen in figure 4(*a*). Similarly, the potential on dot D1 is also a sawtooth as a function of V_A, but with the opposite phase. The amplitude of each of these sawtooth oscillations is calculated to be 100 μV. It is this voltage which must force an electron in the output half-cell to move from D4 to D3. Since the potentials on D1 and D2 act as additional gate voltages for D3 and D4, the honeycomb of the output half-cell will shift in response to potential changes in the input half-cell. The working point of the output half-cell (V_C, V_D) is set close to the border separating the $(0, 1)$ and $(1, 0)$ hexagons. For QCA operation we must have a shift that is sufficient to move the honeycomb border from one side of this working point to the other, representing a switch of an electron in the output half-cell. This switching in the output half-cell will be detected by the two electrometers, where the conductance of one electrometer will increase as an electron leaves its adjacent dot, while the conductance of the other electrometer will decrease as an electron enters its adjacent dot. The experimental measurements confirm this behaviour, as shown in figure 6, which plots the conductance through the input half-cell, together with the conductance through each electrometer as a function of the input voltages $V_B = -V_A$. The peak in the conductance through the input half-cell, seen in figure 6(*a*) as V_B increases, indicates that an electron has moved from D1 to D2. As the electron switches in the input half-cell the electrometer conductances shift in opposite directions, a shift down for the top electrometer of figure 6(*b*) and a shift up for the bottom electrometer of figure 6(*c*). This indicates that an electron has moved from D4 to D3 as expected because of the electron switch in the input half-cell. This confirms the polarization change required for QCA operation.

Using the electrometer signal of figure 6(*b*) we can calculate the potential on D3 as a function of the input differential voltage. This is plotted in figure 7(*a*) together with the theoretically calculated potential at a temperature of 75 mK. Although at a temperature of 0 K the potential changes are abrupt, the observed potential shows the effects of thermal smearing, and theory at 75 mK shows good agreement with experiment. The heating of the electron system to temperatures above that of the dilution refrigerator is probably due to the applied excitation voltage and noise voltages coupled into the sample by the leads. This effect is commonly seen in measurements of this type [11]. Figures 7(*b*) and 7(*c*) plot the theoretical excess charge on each of the dots in the input and output half-cells at 75 mK. This shows an 80% polarization switch of the QCA cell, and the polarization change can be further improved with an increase in the capacitances coupling input and output half-cells.

3. Summary

A device paradigm based on QCA cells offers the opportunity to break away from FET-based logic and to exploit the quantum effects that come with small size. In this new paradigm, logic levels are no longer encoded as voltages but as the position of electrons within a quantum

dot cell. QCA cells are scalable to molecular dimensions, and the performance improves as the size shrinks. A QCA cell with molecular dimensions should operate at room temperature since the energy spacings of the dot states will be larger than kT, even at 300 K. Using aluminium island dots, with aluminium oxide tunnel junctions, we have demonstrated the operation of a QCA cell. The cell exhibits a bistable distribution of electrons, and the polarization of the cell can be switched by externally applied bias voltages.

Acknowledgments

This work was supported in part by the Defense Advanced Projects Agency, Office of Naval Research (Contract N00014-95-1-1166) and the National Science Foundation.

References

[1] Lent C S, Tougaw P D, Porod W and Bernstein G H 1993 *Nanotechnology* **4** 49
[2] Lent C S and Tougaw P D 1997 *Proc. IEEE* **85** 541
[3] Lent C S and Tougaw P D 1993 *J. Appl. Phys.* **74** 6227
[4] Tougaw P D and Lent C S 1994 *J. Appl. Phys.* **75** 1818
[5] Tougaw P D and Lent C S 1996 *J. Appl. Phys.* **80** 4722
[6] Fulton T A and Dolan G H 1987 *Phys. Rev. Lett.* **59** 109
[7] Orlov A O, Amlani I, Bernstein G H, Lent C S and Snider G L 1997 *Science* **277** 928
[8] Likharev K K 1988 *IBM J. Res. Dev.* **32** 144
[9] Pothier H, Lafarge P, Orfila P F, Urbina C, Esteve D and Devoret M H 1991 *Physica* B **169** 573
[10] Amlani I, Orlov A O, Snider G L, Lent C S and Bernstein G H 1997 *Appl. Phys. Lett.* **71** 1730
[11] Lafarge P, Pothier H, Williams E R, Esteve D, Urbina C and Devoret M H 1991 *Z. Phys.* B **85** 327